JOURNAL OF MATERIALS SCIENCE 25 (1990) 575–579

A mechanism for sub-surface median crack initiation in glass during indenting and scribing

WEILI CHENG, IAIN FINNIE
Department of Mechanical Engineering, University of California, Berkeley, California 94720, USA

The initiation of sub-surface median cracks in glass during indenting and scribing is studied. It is shown that the zone of intense deformation under the tool introduces a weak singularity which may have a strong influence on crack initiation. When combined with a crack nucleus, which need only be of the order of the dimensions of the glass network, the weak singularity allows the threshold load for median cracking to be estimated. This estimate is shown to be in good agreement with experimental observations. The analysis explains the sudden transition from brittle to ductile behaviour in glass and also provides a possible explanation for the origin of the elusive "Griffith flaws".

1. Introduction

It is a familiar observation that glasses, and other solids which are normally thought of as brittle, may show ductile behaviour without cracking when indented, scribed or cut under very low loads. The threshold at which cracking occurs is thus of major importance if one is contemplating the ductile machining or grinding of glass [1]. As a first step in attempting to predict the transition from ductile to brittle behaviour, we consider the initiation of a median crack under the indentor shown in Fig. 1. The compacted and sheared zone under the indentor, often referred to as the "plastic" zone, is enclosed schematically by the dashed line in the figure. The detailed mechanisms of deformation in this zone are still not well understood but it seems clear that the irreversible deformation occurs due to shear bands rather than homogeneous plastic deformation. The propagation of a median crack once it is initiated has been treated extensively in the literature using the methods of fracture mechanics. However, the question of initiation is more complex and has received less attention.

The first model proposed for median crack initiation was based on pre-existing flaws [2]. However, the size of the flaws predicted for some materials was so large that they should have been detectable. Another approach which does not invoke pre-existing flaws was then proposed by Hagan [3]. This model uses dislocations piling up on a shear band formed along the boundary of the plastic zone as the mechanism for crack initiation. In later work by Chiang *et al.* [4], an attempt was made to express crack initiation in terms of the size and geometric configuration of the crack nucleus and the surrounding stress field. However, quantitative prediction of initiation was not obtained because of the uncertain nature of the crack nucleus.

In this paper we take a different approach to those presented earlier for crack initiation. As a starting point we demonstrate that the intersection of two shear bands introduces a weaker singularity than that due to a crack or Griffith type of flaw [5]. We will refer to the weak singularity as an F-flaw to distinguish it from the Griffith or G-flaw so often invoked in linear elastic fracture mechanics. The order of the singularity for the F-flaw depends on the intersection angle of the shear bands and has a great influence on crack initiation. The only additional condition necessary for crack initiation is the presence of a crack nucleus along the future cracking plane adjacent to the F-flaw. As will be shown later, the predictions are quite insensitive to the choice of the nucleus dimension which needs only be of the order of the size of the open spaces in the glass network. This leads to the prediction of a traditional G type of singularity at the end of the crack nucleus. Because our work is motivated by an interest in processes in which an indentor is moved along the surface, such as scribing, machining and grinding, we use a plane strain analysis. This assumption is also implicit in Hagan's model [3].

2. Analysis of crack initiation due to F-flaws

To begin with, we consider a pair of shear bands, which intersect at a point on the median plane as shown in Fig. 1. The arrows in Fig. 1 indicate the direction of relative motion of the material along the shear bands and the direction of shear forces, which as a result of the indentation load, act on each side of the shear planes. In reality, the chance that two shear bands intersect exactly at a point or along a line in a three-dimensional body is very small. Thus, the intersection is developed when a longer shear band blocks the propagation of a shorter one. Because shear bands always form before crack nucleation, we first consider shear band intersection with no crack nucleation. We make a virtual separation along the shear bands and include both tangential and normal surface tractions as shown in Fig. 2. It is seen that the shear traction

0022–2461/90 $03.00 + .12

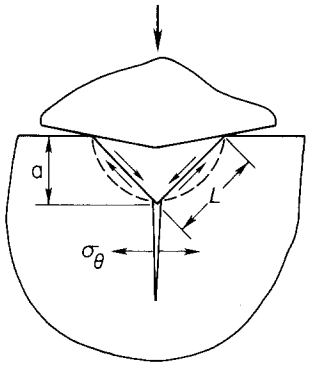

Figure 1 Median crack initiation from two shear bands. The zone of intense compaction and shear under the tool is shown enclosed by a dashed line.

acting on the lower part of the body produces a compressive stress along the median plane and the normal traction produces a tensile stress. The lower part of the figure corresponds to a V-notched body which accommodates the relative slip along both of the shear bands. Thus, the presence of a crack nucleus at the notch tip will initiate a median crack if the tensile stress at the notch tip is large enough. This is exactly what one might have expected from Hagan's model if two shear bands and the total normal tractions were all taken into account. It is worth noting that Hagan [3] also pointed out the possibility of crack initiation due to the wedging action of the deformed zone, which is the first step to the understanding of F-flaws.

In reality, shear bands are not straight and many intersecting points may form along the elastic/plastic boundary. Therefore, each intersecting point with a V-notch-like tip corresponds to an F-flaw which induces a singularity. Depending upon the stress field, F-flaws at different locations may initiate different types of cracking. In scribing or indentation, those at the bottom of the elastic/plastic boundary are responsible for median cracking and those at other parts of the boundary may be responsible for lateral cracking. F-flaws may also arise from the inhomogeneous structure of materials. By contrast to G-flaws, the F-flaws may have more than two singular points in a two-dimensional body or singular lines in a three-dimensional body. The order of singularity varies between one-half and zero. G-flaws may be considered as a special class of F-flaws whose singularity is exactly equal to one-half. The mechanism we propose for

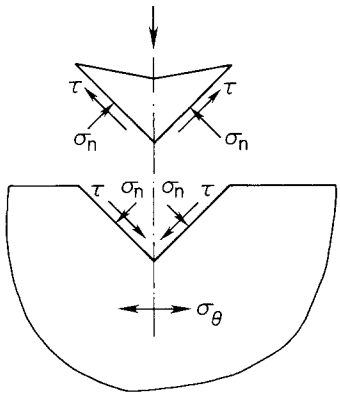

Figure 2 Virtual separation along the two shear bands.

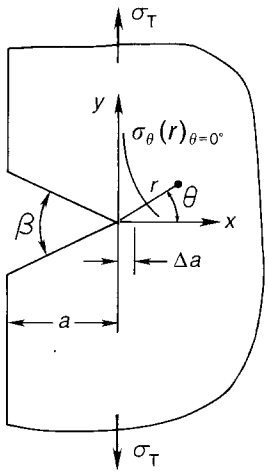

Figure 3 A V-notch in a semi-infinite plane subjected to a remote uniform tension σ_T.

sub-surface crack initiation is based on these F-flaws which may exist as the inhomogeneous structure or may be formed as a result of the intersection of shear bands or other modes of deformation.

As predicted by this mechanism, a sub-surface crack is initiated if the stress intensity factor for the F-flaw, combined with a crack nucleus with a dimension of the order of the network spacing in the glass, reaches a critical value which is sufficient to produce a Griffith crack. We present here a simple approach to calculate the stress intensity factor. Consider a semi-infinite plate with a V-notch subjected to a remote symmetric loading as shown in Fig. 3. The depth of the notch, a, corresponds to the size of an F-flaw formed by two shear bands. The hoop stress ahead of the notch tip for $\theta = 0°$ can be expressed as [6]

$$\sigma_\theta(r) = K_I^p(r)^{p-1}/(2\pi)^{1/2} \quad (1)$$

in which r is the distance from the tip, and $p - 1$, the order of singularity, is shown in Fig. 4 as a function of the notch angle. For a small virtual crack introduced at the notch tip, the expression for the stress intensity factor for an edge crack with an arbitrary crack face loading given in [7] may be used to yield

$$K_I = (2/\pi)^{1/2} \int_0^{\Delta a} \sigma_\theta(r)(\Delta a - r)^{-1/2} dr \quad (2)$$

assuming that Δa as shown in Fig. 3 is much less than the equivalent length of the notch a. Equation 2 can also be derived for a centre crack [8] or any other crack configurations subjected to mode I loading

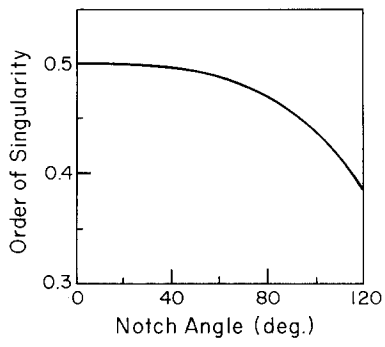

Figure 4 The order of the singularities of F-flaws as a function of the notch angle β.

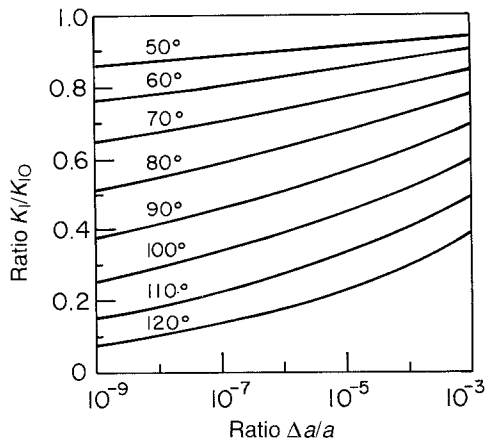

Figure 5 Ratios of K_I/K_{Io} for F-flaws with different included angles and $\Delta a/a$ ratio.

conditions. Substitution of Equation 1 into Equation 2 leads to

$$K_I = (2/\pi)^{1/2} \int_0^{\Delta a} [K_I^p/(2\pi)^{1/2}](r)^{p-1}(\Delta a - r)^{-1/2}dr$$
$$= K_I^p \int_0^{\Delta a} (r)^{p-1}/[\pi(\Delta a - r)^{1/2}]dr$$
$$= K_{Io}\lambda(\beta)(\Delta a/a)^{p-1/2}f(p) \quad (3)$$

where the weak stress intensity factor is defined as

$$K_I^p = 1.12\lambda(\beta)\sigma_T(\pi)^{1/2}(a)^{1-p} \quad (4)$$

and

$$f(p) = \Gamma(p)\Gamma(1/2)/[\pi\Gamma(p + 1/2)] \quad (5)$$

$$K_{Io} = 1.12\sigma_T(\pi a)^{1/2} \quad (6)$$

In Equation 4, σ_T is a uniform tensile stress, and $\lambda(\beta)$ is a parameter which increases slightly from unity as β increases from zero. The quantity $\lambda(\beta)$ may be estimated by comparing Equation 3 with results given by Hasebe and Iida [9]. When the notch angle $\beta = 0°$, Equation 3 reduces to the conventional stress intensity factor. For $\beta \neq 0°$ the right-hand side of Equation 3 is a function of both the order of the singularity and the $\Delta a/a$ ratio. In fracture analysis of a continuum we never need to consider the physical limitation on how small a crack can be made. However, for F-flaws the size of the virtual crack extension Δa may be as small as the dimension of the smallest possible crack nucleus, i.e. about 2×10^{-10} m (0.2 nm). Fig. 5 shows the ratio K_I/K_{Io} for F-flaws with different included angles. It is seen that the angle of the F-flaw has significant influence on K_I. For scribing, the critical F-flaw size at the median cracking threshold in glass is typically about 1 or 2×10^{-6} m. The estimated K_I for this value of a and the value of Δa quoted earlier with $\beta = 110°$ is about 43% of that for a crack of length a. It can also be seen in Fig. 5 that the estimated K_I is very insensitive to the value of $\Delta a/a$.

As predicted by Equation 3, the stress intensity factor increases after crack initiation from an F-flaw and crack extension always follows. An analysis based on a crack instead of Equation 3 should be used to estimate K_I if the extension of the crack is no longer small compared with the size of the F-flaw.

3. Estimation of crack initiation

The plastic deformation under an indentor or a scribing tool consists of shear and compaction which, as observed by Hagan [10], depends on the composition of the glass. In shear deformation the propagation of shear bands, as suggested by Ernsberger [11], may be achieved by finding a path through the ionically bound regions of the glass. The intersecting points of shear bands introduce F-flaws along the elastic/plastic boundary and the one at the bottom is most critical to median crack initiation. The intersection angle of shear bands after indentation by a Vickers indentor was found to be about 110° [10]. As discussed in the Appendix, the fact that the intersection angle observed in glass is greater than 90° may be explained by taking compaction into account. In this paper the intersection angle of the bands is taken as 110°.

The pressure under indentors has been discussed at length for elastic, plastic and elastic–plastic behaviour. In the present case the formation of shear bands and compaction of glass will probably lead to a relatively uniform stress distribution such as is obtained for non-strain hardening plasticity. This assumption is also implicit in the work of Hagan [3]. Assuming that the two shear bands are straight and both the normal and shear tractions are constant along the shear bands, the normal stress, σ_n, acting on the shear bands shown in Fig. 2 may be expressed in terms of the shear stress and the hardness H (load–projected area of indentation). As shown in Fig. 6, this then allows the equivalent horizontal stress, σ_t, to be written as

$$\sigma_t = H - \tau/[\sin(\beta/2)\cos(\beta/2)] \quad (7)$$

We now consider the contribution of the vertical stress, H, shown in Fig. 6b to the stress intensity factor. Because no remote tension can be directly related to the vertical stress, a simple approximate analysis is presented here. Consider a semi-infinite plane with uniform vertical loading along the notch shown in Fig. 7 as field I. From superposition, field I can be obtained from field II and field III in Fig. 7. These two fields can be further decomposed into four fields shown in the lower part of Fig. 7. The singular stress field corresponding to the vertical stress H can be seen to be only due to fields IIb and IIIa. Stress field IIb leads to a horizontal stress $\sigma_{t2} = -H$. It can be shown that the magnitude of the horizontal

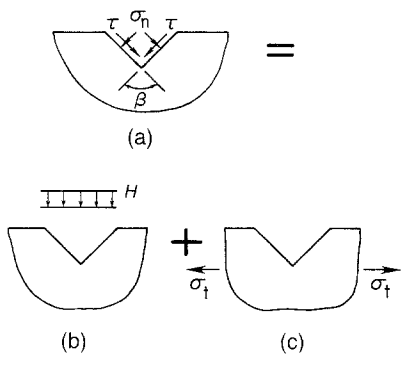

Figure 6 A V-notch formed by two straight shear bands subjected to uniform shear and normal surface traction.

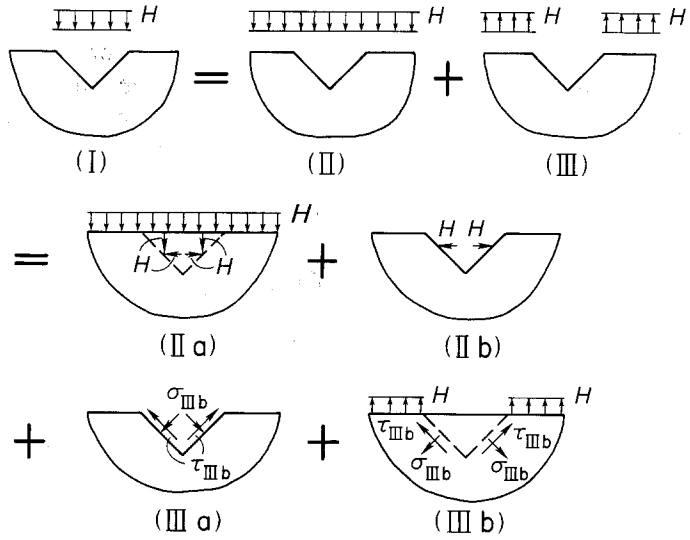

Figure 7 Determination of the equivalent horizontal component due to normal pressure H.

component for stress field IIIa is about $0.3H$ for $\beta = 110°$ [12]. The equivalent horizontal stress for a vertical stress H is thus $\sigma_{t2} + \sigma_{t3} = -0.7H$. From Equation 7 the total equivalent horizontal stress for $\beta = 110°$ becomes

$$\sigma_T = 0.3H - 2.13\tau \quad (8)$$

As mentioned earlier, the presence of a crack nucleus at the notch tip is a necessary condition for crack initiation. The source for crack nucleation is widely believed to be due to the intersection of shear bands, although other mechanisms such as open structure and impurities in glass are also possible. Here we only consider the nucleation due to shear bands because the uncertainty involved in estimation of the shear stress in Equation 8 can be avoided.

Whether or not a shear band is formed in glass by dislocations piling-up is still under debate [13, 14]. However, it is generally agreed that a shear band may act to produce crack nucleation in the same manner as dislocations piling-up. Stroh proposed a criterion [15] for crack nucleation due to piled-up dislocations. This leads to crack nucleation on a plane at 70.5° to the shear band. For initiation of a crack nucleus lying on the median plane, a slight modification of Stroh's analysis using the singularity solution leads to

$$\tau^2 = 3\pi\alpha K_{Ic}^2/32L \quad (9)$$

where L is the length of the shear band shown in Fig. 1 and α is a correction factor for crack nucleation on the medium plane. For $\beta = 110°$, α is about 1.12 and $L = 1.23(2a)^{1/2}$. Substituting Equations 8 and 9 into Equation 3, the critical F-flaw size can be found to be

$$a_{cr} = A(K_{Ic}/H)^2 \quad (10)$$

where A is a dimensionless constant with a value of 51 for $\beta = 110°$. The fracture toughness for soda-lime glass in vacuum is about $0.76\,MN\,m^{-3/2}$ [16] and the measured hardness is about 5 GPa. The predicted critical F-flaw size is then about 1.2×10^{-6} m. The threshold load for a moving Vickers indentor, for which the contact area is approximately half of that for static loading, may be expressed as

$$P_{cr} = 2A^2[K_{Ic}/H]^3K_{Ic} \quad (11)$$

With the same values for K_{Ic}, H and A, the threshold load is estimated to be about 0.014 N. The threshold load obtained by Peter [17] is about 0.05 N using optical observation on soda-lime glass scribed by a Vickers indentor with an edge leading. For the same configuration using an indentor with an included angle smaller than that of the Vickers indentor and a velocity of about 1 cm sec^{-1} we have observed threshold loads between 0.015 and 0.022 N by using a scanning electron microscope to examine cleaved cross-sections.

Because the prediction of the critical F-flaw size and threshold load is based on a plane strain analysis, the obtained results are expected to be more appropriate for scribing than indenting.

4. Discussion

The low fracture strength of bulk specimens of glass, the variability of strength and the effect of specimen size on strength are all consistent with the presence of pre-existing flaws of varying severity. However, these so-called "Griffith" flaws have never been detected directly and their origin has yet to be determined. The present analysis shows that sub-surface median cracks may be initiated from F-flaws as a result of shear bands or other inhomogeneous deformation which introduces a weak singularity. Whether an F-flaw initiates a median crack is closely related to the local deformation or the inherent structure of the material at the tip of the flaw. A procedure is presented to estimate the initiation threshold from crack nuclei produced by shear bands. A curious but fortunate result is that the estimated stress intensity factor for an F-flaw shows a very weak dependence on the size of the crack nucleus. For example, for a three-fold increase in the dimension of the nucleus, the stress intensity factor estimated from Equation 3 changes by only 5% for $\beta = 90°$. The dimension Δa required to provide a stress intensity factor comparable to that of a Griffith flaw of depth a is only several tenths of a nanometre which is about the size of the open dimensions of the glass network. Thus, there is no difficulty in providing a crack nucleus. Threshold loads are remarkably low and could be exceeded in situations such as placing a glass plate on a flat surface

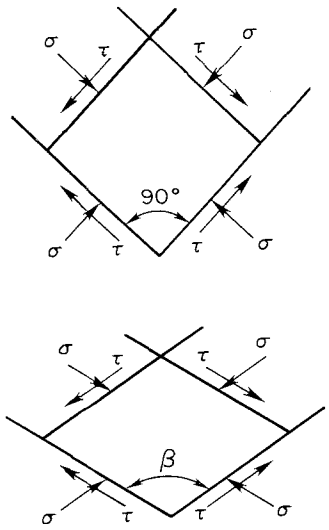

Figure 8 Permanent deformation due to both shear and compaction.

covered with dust particles or rubbing a glass surface with a cloth containing small particles. The median cracks produced in these cases would not be detected by surface examination. A question which needs to be answered is the extent to which these median cracks may grow if residual stresses are present and if water vapour can enter the crack.

Finally, we note that the mechanism discussed provides a satisfactory explanation of the abruptness of the brittle–ductile transition which is observed when glass is loaded by smaller and smaller particles, as in erosion [18]. This is inconsistent with a pre-existing distribution of flaws but rather suggests that the flaws arise from the impact forces produced by erosion.

Acknowledgement

This work was supported by the Lawrence Livermore National Laboratory of the University of California, Livermore, California.

Appendix

The observation that the intersection angle of two shear bands is larger than 90° confirms that the permanent deformation under an indentor undergoes both shear and compaction.

In plastic deformation there is no volume change and the shear bands always intersect at 90°. For soda-lime glass, however, the volume is not conserved if the pressure is high enough. Consider an element, as shown in Fig. 8, which is enclosed by two pairs of parallel shear bands. When the pressure in the vertical direction is high enough, compaction occurs which leads to an increase of the intersection angle, β. It can be seen from Fig. 8 that the change of the volume from V_0 to V and the change of the angle β are related by

$$(V_0 - V)/V_0 = 1 - \cos(\beta - 90°) \quad \text{(A1)}$$

It is of interest to note that the increase in the angle of the shear bands cannot be attributed to a "Coulomb type" increase of the shear stresses. This occurs in granular solids and results in shear bands which intersect at less than 90° [19].

References

1. J. H. GIOVANOLA and I. FINNIE, *J. Mater. Sci.* **15** (1980) 2508.
2. B. R. LAWN and A. G. EVANS, *ibid.* **12** (1977) 2195.
3. J. T. HAGAN, *ibid.* **14** (1979) 2975.
4. S. S. CHIANG, D. B. MARSHALL and A. G. EVANS, *J. Appl. Phys.* **53** (1982) pp. 312–317.
5. A. A. GRIFFITH, Proceedings of the 1st International Congress for Applied Mechanics, Delf, 1924, edited by C. B. Biezeno and J. M. Burgers (J. Wltman, Delf, Holland) p. 55.
6. M. L. WILLIAMS, *J. Appl. Mech. Trans. ASME* **74** (1952) 526.
7. W. CHENG and I. FINNIE, *Engng Fract. Mech.* **31** (1988) 201.
8. J. R. RICE, *Int. J. Solid Struct.* **8** (1972) 751.
9. N. HASEBE and J. IIDA, *Engng Fract. Mech.* **10** (1978) 773.
10. J. T. HAGAN, *J. Mater. Sci.* **15** (1980) 1417.
11. F. M. ERNSBERGER, *Glass Sci. Technol.* **5** (1980) 1.
12. H. TIMOSHENKO and J. N. GOODIER, in "Theory of Elasticity", 3rd Edn (McGraw-Hill, New York, 1970).
13. N. P. BANSAL and R. H. DOREMUS, "Handbook of Glass Properties", (Academic, Orlando, Florida, USA, 1986) p. 371.
14. J. J. GILMAN, *J. Appl. Phys.* **44** (1973) 675.
15. A. N. STROH, *Adv. Phys.* **6** (1957) 418.
16. S. W. FREIMAN, T. L. BAKER and J. B. WACHTMAN Jr, "A Computerized Fracture Mechanics Database for Oxide Glasses", NBS Technical Note 1212 (US National Bureau of Standards, Gaithersburg MD, USA, 1985).
17. K. PETER, *Glastech. Ber.* **37** (1964) 333.
18. G. L. SHELDON and I. FINNIE, *Trans. ASME* **88B** (1966) 387.
19. V. V. SOKOLOVSKII, in "Statics of Granular Media" (Pergamon Student Editions, 1965).

Received 4 October 1988
and accepted 22 February 1989